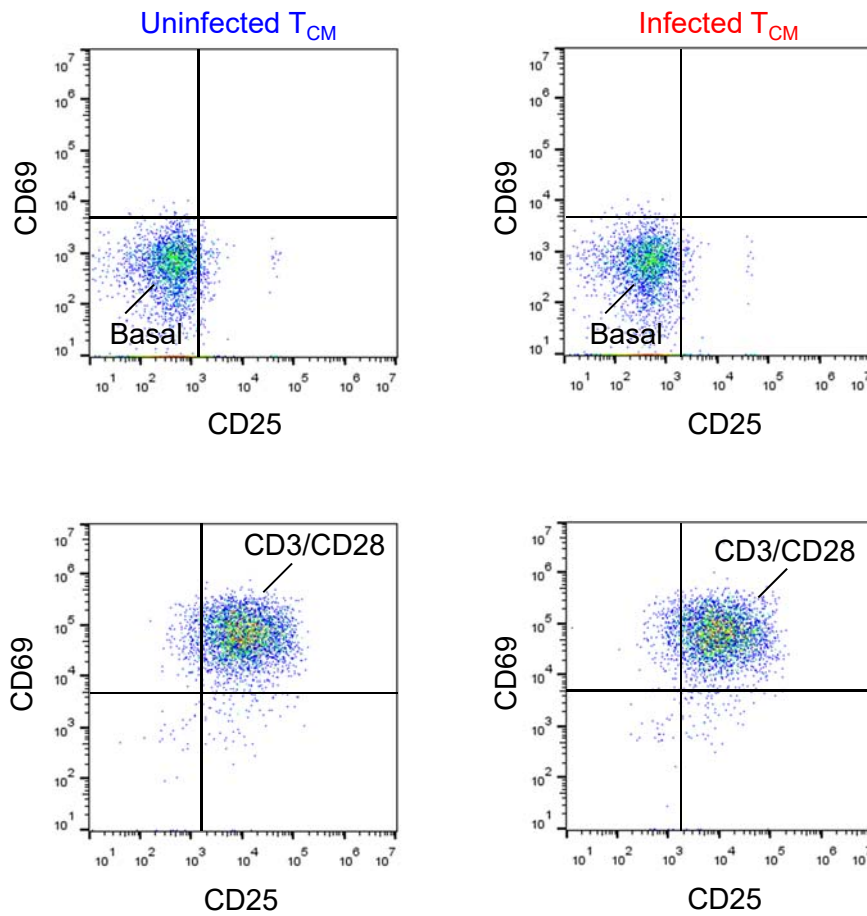


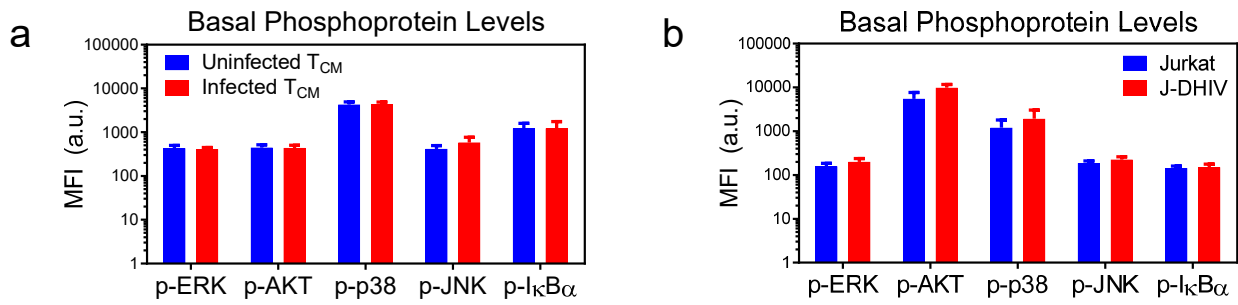
Systems analysis of latent HIV reversal reveals altered stress kinase signaling and increased cell death in infected T cells

Linda E. Fong, Endah S. Sulistijo, and Kathryn Miller-Jensen*

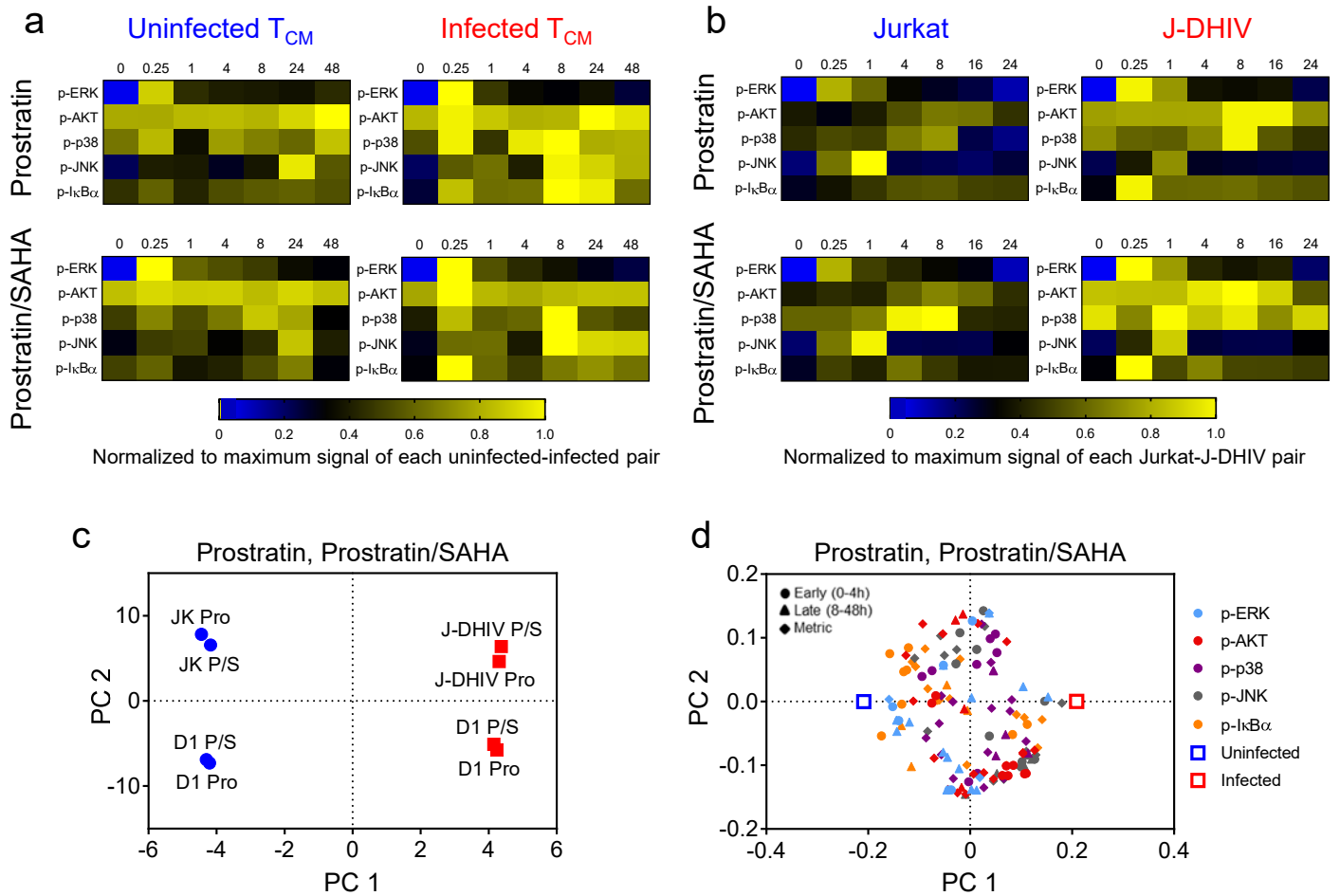
Supplementary Information



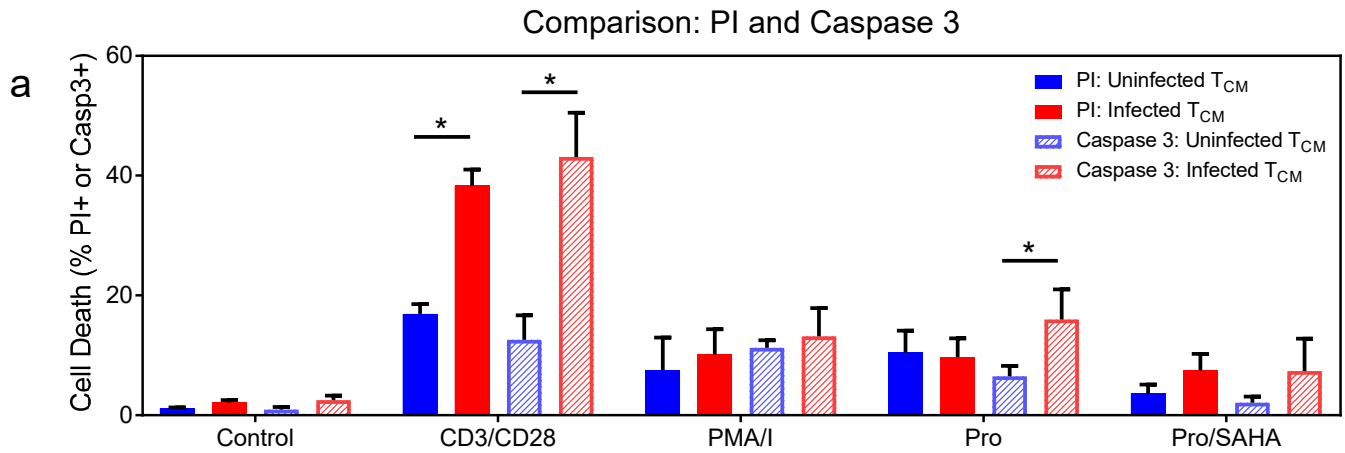
Supplementary Figure S1. CD3/CD28 stimulation induces T cell activation similarly in uninfected and latently infected cells. Uninfected and infected primary cultured CD4⁺ T_{CM} populations were co-stained for the activation markers, CD25 and CD69, in the basal state and following 48 hours of CD3/CD28 stimulation and measured by flow cytometry.



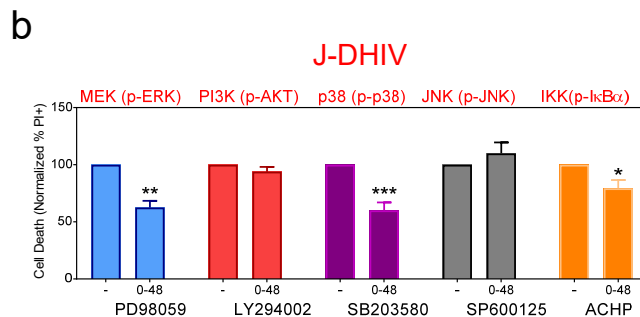
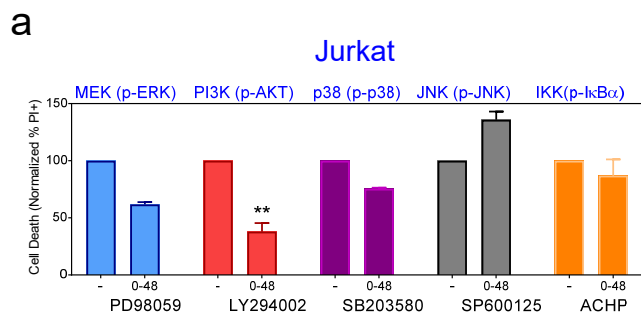
Supplementary Figure S2. Latently infected cells and uninfected cells show similar levels of basal phosphorylation. (a-b) Basal phosphorylation levels of ERK, AKT, p38, JNK, and I κ B α as measured by bead-based immunoassay for uninfected (blue) and infected (red) primary T_{CM} cells from one representative donor (a) and for Jurkat (blue) and J-DHIV (red) T cells (b). Data are plotted as means \pm standard deviations (SD) of at least 3 biological replicates.



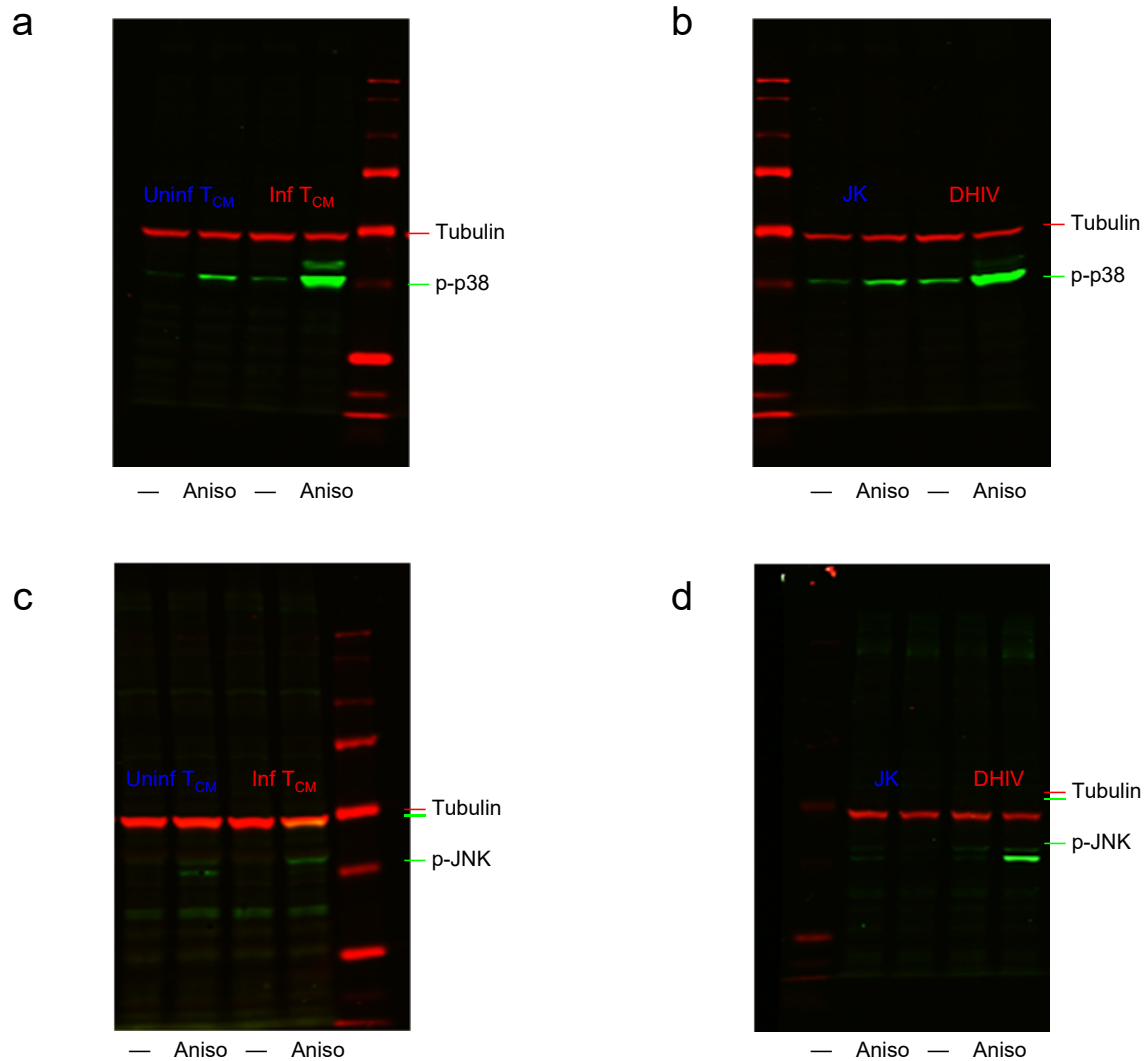
Supplementary Figure S3. Phospho-signaling differences following stimulation with prostratin +/- SAHA classify uninfected versus latent HIV-infected T cells in a PLS-DA model. (a-b) Heatmaps of phospho-protein time courses measured by bead-based immunoassay following Prostratin or Prostratin/SAHA stimulation in uninfected (blue) and infected cells (red) for (a) primary T_{CM} cells from one donor and (b) Jurkat and J-DHIV cell lines. Phospho-signals are normalized to the maximum level of each uninfected and infected pair. Phospho-signals were measured in biological triplicate and 90% of measurements had an SD < 15%. Raw data provided in **Supplementary Datasets S9-S12**. (c-d) PLS-DA model comprising three principal components was calculated from phospho-protein time course data presented in (a-b) for uninfected and infected T cells treated with Prostratin and Pro/SAHA (R₂X = 0.71, R₂Y = 0.99, Q₂ = 0.82). (c) Model scores of uninfected (blue) and infected (red) cells for both primary T_{CM} cells and Jurkat/J-DHIV cell lines projected onto PC1 versus PC2. (d) Model loadings of phospho-proteins and host-cell classification (uninfected, blue; infected, red) projected onto PC1 versus PC2 for each phospho-protein (see legend for color codes). Early time points (0-4 hours), circles; late time points (8-48 hours), triangles; time-dependent metrics, squares.



Supplementary Figure S4. PI measurements correlate closely to apoptosis levels as measured by cleaved caspase 3 immunostaining. (a) Uninfected and infected primary T_{CM} cells were treated with the indicated stimuli and cell death was assayed via PI staining (same as data presented in **Figure 4a**) or cleaved caspase 3 immunostaining and measured by flow cytometry. Percentage of positively stained cells at 24 hours was measured in biological duplicate. Bar graph depicts means \pm SD.



Supplementary Figure S5. Pathway inhibition in Jurkat/DHIV cell lines emphasizes the role of p38 for cell death regulation. Cell death in the presence of the indicated inhibitor was measured in response to stimulation with CD3/CD28 in Jurkat (a) and J-DHIV cells (b) by flow cytometry and normalized to the uninhibited control. Percentage of PI⁺ cells was measured in biological triplicate. Data are presented as means \pm SD. Student t-tests were conducted to determine significance (***, $p \leq 0.001$; **, $p \leq 0.01$, * $p \leq 0.05$, ns, $p > 0.05$).



Supplementary Figure S6. Western blots show that latently infected cells exhibit increased signaling following treatment with the p38 and JNK agonist anisomycin. (a-d) Western blots for p-p38 (a-b) and p-JNK (c-d) expression with and without anisomycin treatment in uninfected (blue, left 2 lanes) and infected (red, right 2 lanes) primary T_{CM} cells (a,c) and Jurkat (JK) /J-DHIV cells (b,d). Antibodies from Cell Signaling Technologies: Anti- p-p38 (Cat # 9211S)⁴⁶ and Anti- p-JNK (Cat # 9251S)⁴⁶ Antibody from Abcam: Anti- alpha Tubulin Loading Control (Cat # ab89984)⁴⁷

Phospho-protein	Residue Measured	Relevance to HIV
p-ERK	Thr ²⁰² /Tyr ²⁰⁴ Thr ¹⁸⁵ /Tyr ¹⁸⁷	<ul style="list-style-type: none"> ERK phosphorylation of the transcription factor LSF reduces binding at the HIV LTR, thereby decreasing recruitment of YY1 and histone deacetylases, to promote HIV reactivation (Ylisastigui, L. J Virol. 2005). ERK phosphorylates transcription factors c-Myc, AP-1, NF-κB, IL-6, ATF-2, and ELK-1 which contribute to HIV expression (Yang, X. J Bio Chem. 1999). ERK inhibitor U0126 blocks both P-TEFb recruitment to the HIV LTR, reducing HIV transcription (Briant, L. J Immuno. 1998).
p-AKT	Ser ⁴⁷³	<ul style="list-style-type: none"> SAHA induced acetylation and NF-κB activation is AKT-dependent. Treatment of primary cells with PI3K inhibitor Wortmannin has shown no effect on HIV reactivation (Contreras, X. PLoS Pathogens. 2009). Nef-mediated HIV reactivation is associated with AKT activation. Treatment with protease inhibitors, but not RTIs, can block this AKT activation. (Kumar, A et al. Sci Rep. 2016)
p-p38	Thr ¹⁸⁰ /Thr ¹⁸²	<ul style="list-style-type: none"> p38 phosphorylation increases LSF occupancy at LTR, promoting HIV transcription and p38 inhibition blocks the ability of YY1 to inhibit HIV activation (Ylisastigui 2005).
p-JNK	Thr ¹⁸³ /Tyr ¹⁸⁵	<ul style="list-style-type: none"> Treatment of primary cells with JNK Inhibitor V, AS601245, prevents HIV reactivation (Wolschendorf, F. J Virol. 2012).
p-IκBα	Ser ³² /Ser ³⁶	<ul style="list-style-type: none"> IKK-dependent phosphorylation and degradation of IκBα leads to subsequent release and nuclear translocation of the NF-κB transcription factor, which positively regulates HIV transcription (Brooks, D. PNAS. 2003). In CCL19-resting CD4+ T cells, inhibition of AP-1 and NF-κB inhibits HIV integration. (Saleh, S et al. Retrovirology. 2016)

Supplementary Table S1. Phosphorylation sites and phospho-protein involvement in HIV activation and expression.

Estimated Latent Percentage	Donor 1	Donor 2	Donor 3
Fig. 1e	17.3 ± 5.8	42.9 ± 1.3	48.1 ± 1.8
Fig. 1f	36.1 ± 3.7	36.9 ± 2.9	45.2 ± 2.1
Fig. 3a, c	17.3 ± 5.8	42.9 ± 1.3	48.1 ± 1.8
Fig. 3b, d	36.1 ± 3.7	36.9 ± 2.9	45.2 ± 2.1
Fig. 4a-b	17.3 ± 5.8	42.9 ± 1.3	48.1 ± 1.8
Fig. 4c-d	36.1 ± 3.7	36.9 ± 2.9	45.2 ± 2.1
Fig. 4e-f	22.6 ± 1.3 34.4 ± 4.5 43.7 ± 3.2	32.7 ± 3.3 55.6 ± 3.7 47.0 ± 4.8	
Fig. 5a		39.2 ± 1.7	
Fig. 5a-d	17.3 ± 5.8	42.9 ± 1.3	48.1 ± 1.8
Fig. 5e-f	22.6 ± 1.3 34.4 ± 4.5 43.7 ± 3.2	32.7 ± 3.3 55.6 ± 3.7 47.0 ± 4.8	
Fig. 6c, g, k		54.2 ± 6.9	
Fig. 6f, j		36.2 ± 2.6	
S2 Fig. a	17.3 ± 5.8 36.1 ± 3.7	42.9 ± 1.3 36.9 ± 2.9	48.1 ± 1.8 45.2 ± 2.1
S3 Fig. a-d	25.97 ± 0.7		
S4 Fig. a	25.97 ± 0.7		
S4 Fig. b	17.3 ± 5.8 36.1 ± 3.7 25.97 ± 0.7		
S6 Fig. a-f		54.2 ± 6.9	
S7 Fig. a-b		36.2 ± 2.6	
S8 Fig. a-b	36.1 ± 3.7	36.9 ± 2.9	45.2 ± 2.1
S8 Fig. c-d	25.97 ± 0.7		

Supplementary Table S2. Estimated percentage of latent cells per donor per experiment based on the response to CD3/CD28 stimulation.